We are IntechOpen, the world's leading publisher of Open Access books
Built by scientists, for scientists

6,900
Open access books available

185,000
International authors and editors

200M
Downloads

154
Countries delivered to

Our authors are among the

TOP 1%
most cited scientists

12.2%
Contributors from top 500 universities

CLARIVATE ANALYTICS
BOOK CITATION INDEX
INDEXED

WEB OF SCIENCE™

Selection of our books indexed in the Book Citation Index
in Web of Science™ Core Collection (BKCI)

Interested in publishing with us?
Contact book.department@intechopen.com

Numbers displayed above are based on latest data collected.
For more information visit www.intechopen.com

Applications of Computational 3D–Modeling in Organismal Biology

Christian Laforsch[1,2], Hannes Imhof[1,2], Robert Sigl[1,2],
Marcus Settles[3], Martin Heß[2,4] and Andreas Wanninger[5]
[1]Department of Biology II, Ludwig-Maximilians-University Munich,
[2]GeoBioCenter, Ludwig-Maximilians-University Munich,
[3]Institute of Radiology, Technical University of Munich,
[4]Department of Biology I, Ludwig-Maximilians-University Munich,
[5]Dept. of Integrative Zoology, Faculty of Life Sciences, University of Vienna,
[1,2,3,4]Germany
[5]Austria

1. Introduction

Understanding the interrelations between form, function and evolution has traditionally been a major goal in organismal biology. In former times only line drawings or illustrations have been used to display the fascinating variety of body shape and the underlying functional morphology of living animals. A textbook example for scientific illustrations is still the artwork "Kunstformen der Natur", published by Ernst Haeckel between 1899 and 1904. However, the nature of most of his drawings is art rather than an accurate scientific description of the displayed creatures. When Francesco Stelluti showed details of honey bees in 1625 by using the first simple optical microscope it became obvious that technical improvement leads to substantial progress in elucidating the secrets of nature (Bardell, 1983). Along with the development of photographic and microscopic techniques the quality of biological drawings and illustrations increased, but still only two-dimensional images of dissected or sectioned species were available in order to illustrate the structural nature of organisms. However, to analyse the spatial arrangement of both macroscopic and microscopic three-dimensional biological structures the study of two-dimensional data sets alone is often not sufficient. Given that three-dimensional visualizations facilitate the understanding of the spatial assembly of the object of interest (OOI) and in addition often provide novel information, manual graphical reconstructions were generated prior to the era of computational 3D-imaging (Verraes, 1974). Although scientists gained a deeper understanding about complex morphologies and even the ontogeny of organisms by the application of this labour-intensive approach, it is still limited by the plane of the histological sections. The rapidly advancing field of digital imaging techniques combined with an increase in computational capacity enabled the implementation of computerized 3D-reconstructions, which in turn has opened new avenues in biological sciences (Fig. 1). The entire process of 3D-reconstruction starts from data acquisition by the use of a variety of digital imaging techniques. The obtained image

stacks made up of digital pixels are subsequently processed by the appropriate software to model the OOI with high geometric accuracy, resulting in an interactive virtual clone of the selected biological structure. The anatomy of the OOI can be explored by choosing any virtual cutting plane through the raw data stack. Finally, the derived 3D-model can be viewed from different angles and translucent depictions even allow displaying the spatial arrangement of several structures simultaneously. The computerized 3D-models of organs, tissues and cells could then give further insights into the relationship between macroscopic structures such as bones, the connection between microscopic structures such as neuronal networks and the distribution of single components in a tissue such as the distribution of a neurotransmitter in the brain or even the expression pattern of a single gene. In addition, it facilitates precise volume and surface area measurements (Salisbury, 1994).
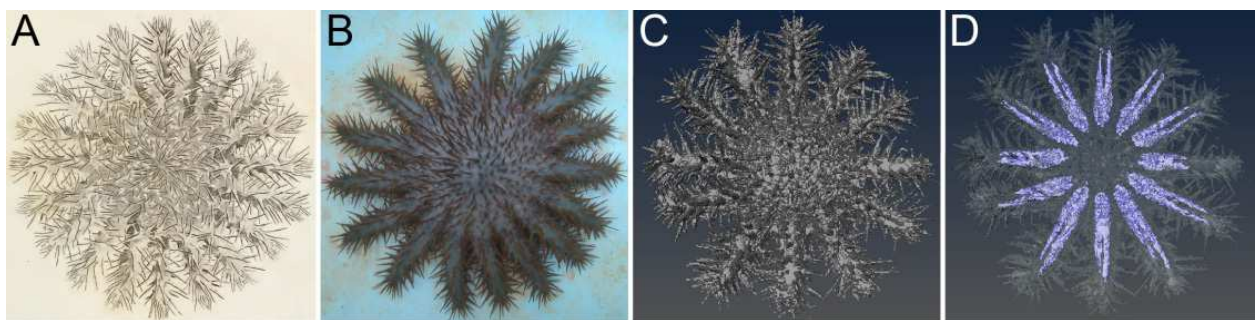

Fig. 1. From drawings to 3D-models, development of imaging techniques.
A Classical drawing of *Acanthaster planci* (Plate 61 of Ellis, J. and Solander, D.: The natural history of many curious and uncommon zoophytes collected from various parts of the globe. Published in 1786 by Benjamin and Son at Horace's Head, Fleet Street.). **B** Digital image of *A. planci.* **C** 3D-model of an *A. planci* individual obtained from MRI-image stacks showing the outer morphology (body wall). **D** 3D-model of an *A. planci* individual obtained from MRI-image stacks offering insights into the inner morphology by showing transparent body wall and pyloric caeca (blue).

State-of-the-art imaging techniques provide not only spatial information but they may also carry multi-dimensional information including time (e.g., live cell imaging) or spectral channels. Another major advantage is that, especially for macroscopic applications, scanner-based non-invasive virtual sectioning techniques (e.g., CT, MRI) have been developed for diagnostics and anatomical investigations.

Depending on the underlying scientific question careful considerations are necessary to choose the appropriate digital imaging method. For instance, soft tissues are best depicted using magnetic resonance imaging (MRI), whereas calcareous and bony structures are best displayed using X-ray computed tomography (CT). For small species or investigations on the cellular level different microscopy techniques such as confocal laserscanning microscopy (CLSM) are frequently used to obtain three-dimensional datasets. For micro-structural and morphological studies, conventional histological sectioning followed by 3D-reconstruction is still an indispensable methodology. Here, a selection of several imaging techniques to generate computerized 3D-reconstructions is presented and their fields of application in organismal biology are illustrated.

2. Histological and ultrastructural analysis based on physical sectioning

The prerequisite for this labour-intensive and time-consuming method is embedding and sectioning of organisms or tissues of interest, after appropriate fixation. Thus, the specimen represents a "snapshot" of the living structure as close to its *in vivo* state as possible. Depending on size and consistency (e.g., transparency, rigidity, biochemical composition, etc.) of the biological objects and according to the requirements of the scientific objectives concerning resolution, contrast and spatial precision, different preparation and imaging methods have to be chosen.

If micro-CT (section 4.1), micro-MRI (section 4.2) or optical sectioning microscopy (CLSM, section 3) are not available or not applicable to achieve the desired quality of data, the volume of interest (VOI) has to be cut physically into a most complete series of plane slices and imaged step by step. Subsequently, these images need to be aligned, segmented and reconstructed.

Generalized flowchart for computer-based 3D-reconstructions from section series

---

Step 1. **Procurement** of living biological material (from natural habitat or from culture).

Step 2. If necessary **dissecting** of the organ/tissue to be investigated (after relaxation and euthanization in case of animals).

Step 3. Chemical **fixation** (e.g., formalin, glutaraldehyde, osmiumtetroxide); pH and osmolarity have to be adjusted to minimize shrinkage/swellings. **Decalcification** if needed (calcified bones or shells may damage the knifes).

Step 4. **Embedding** (inclusion or infiltration; e.g., agarose, kryo kits, historesin, epoxy resin).

Step 5. **Trimming** of the cutting surface, considering the orientation of the structure.

Step 6. **Cutting** with microtome (using e.g., steel/glass/diamond knifes) or by ion beam milling. **Mounting** slices on glass slides or TEM grids.

Step 7. **Staining** or "contrasting" slices (e.g., histochemical dyes, immunostaining, heavy metals – in certain cases this step is performed prior to embedding).

Step 8. **Digital imaging** of slices or of block surfaces (both light or electron microscopy); saving of raw data and generation parameters.

Step 9. Digital **preprocessing** of the raw data (e.g., autoscaling, unsharp masking, deconvolution).

Step 10. **Alignment** of image stacks (rigid or elastic registration) and defining voxel size.

Step 11. **Segmentation** of substructures (manually or semi-automatically, e.g., via thresholding).

Step 12. **Rendering** (volume rendering or surface rendering after triangulation).

Step 13. **Morphometry** if required (e.g., volumetry, measuring distances/angles, detecting and counting repetitive structural units).

Step 14. **Presentation**/publication of selected views or interactively manipulable 3D-models (see e.g., Ruthensteiner & Heß, 2008).

Whereas steps 1-3 are common in invasive visualization techniques, the consecutive steps 4-8 are exclusively applied in histological and ultrastructural analyses based on physical sectioning. The subsequent process from digital processing of the raw data (step 9) to the presentation of a 3D-model (step 14) is identical, regardless which method of data

acquisition was applied. Among these steps alignment (step 10) and segmentation (step 11) are crucial to obtain precise volume data from the OOI.

Alignment

For any 3D-reconstruction – in particular when using physical sectioning – image alignment (= image registration) plays a decisive role. To obtain an accurate positioning of all point measurements in the 3D-coordiante system, it is important to match neighbouring 2D image planes as precisely as possible. Simplified, 3 cases can be distinguished: **(1)** Neighbouring planes are correctly aligned *a priori*, because raw data are not acquired in layers (e.g., cone beam micro-CT, MRI with layer selection gradients) or because the acquisition of 2D images is effected without drift from the coherent VOI (e.g., laser scanning microscopy, FIB-FESEM: see section 2.1.2). **(2)** In most cases section series are imaged, whereby the slice orientation with respect to the cutting surface is inevitably lost. Here, subsequent images have to be aligned by transformation and rotation (**rigid registration**). Either this is performed manually by superposition of landmarks in two transparent images (one positive, one negative) until the overlay appears as "flat" as possible, or automatically via iterative shift and cross correlation of two images with an appropriate stop criterion. In this context the correction of some cutting artefacts is possible: by co-embedding tiny polystyrene spheres (e.g., 2 - 20 μm) a compression of slices in cutting direction can be quantified and corrected by unidirectional image stretching, coevally the precise slice thickness can be determined. **(3)** If image distortion is inevitable during raw data acquisition **elastic registration** has to be used. Imaging ultrathin section series by transmission electron microscopy (TEM) may suffer from image distortions generated by electromagnetic lenses, slice compression from cutting and slice deformation in the electron beam. Some partial alignment success can be achieved by computationally intensive image deformation algorithms, such as StackReg in Fiji software (see Thevenaz et al., 1998).

Segmentation

The generation of 3D-views via volume- or surface-rendering requires the identification of structures in the raw data and labelling of the related voxels. This procedure, called "segmentation", can be performed fast and easy in certain cases, either by using the raw data or inverted raw data for volume rendering directly, or by defining thresholds on one or both sides of the relevant intensity range (after contrast enhancement if necessary). The latter enables to extract the structure of interest by a single mouse click (e.g., dark stained object against a bright background in histology, brightly coded bone material against darker soft tissue in CT, fluorescence signal in CLSM). Thresholding, as a rule, produces some artificial border roughness that can be corrected manually or by digital smoothing. Mostly, however, segmentation is a time consuming procedure in which the scientist has to manually label the structures of interest in every single image plane (XY, XZ or/and YZ) using software tools such as a "pencil" or a "polygon lasso". The difficulty in the segmentation of biological structures (e.g., the course of the intestine between adjacent organs or the arborization of a single neuron in the "cable mess" of a brain) lies in the recognition of structure profiles by relative location and inner structure even if contrast is low and in the discrimination from neighbouring structures with similar grey values or without sharp contours. Although some efforts have been made to automatically track structures with adaptive (e.g., Kalman or graph cuts) algorithms having some short-range success (e.g., Jurrus et al., 2006; Yang & Choe, 2009), the human eye and brain seems to be
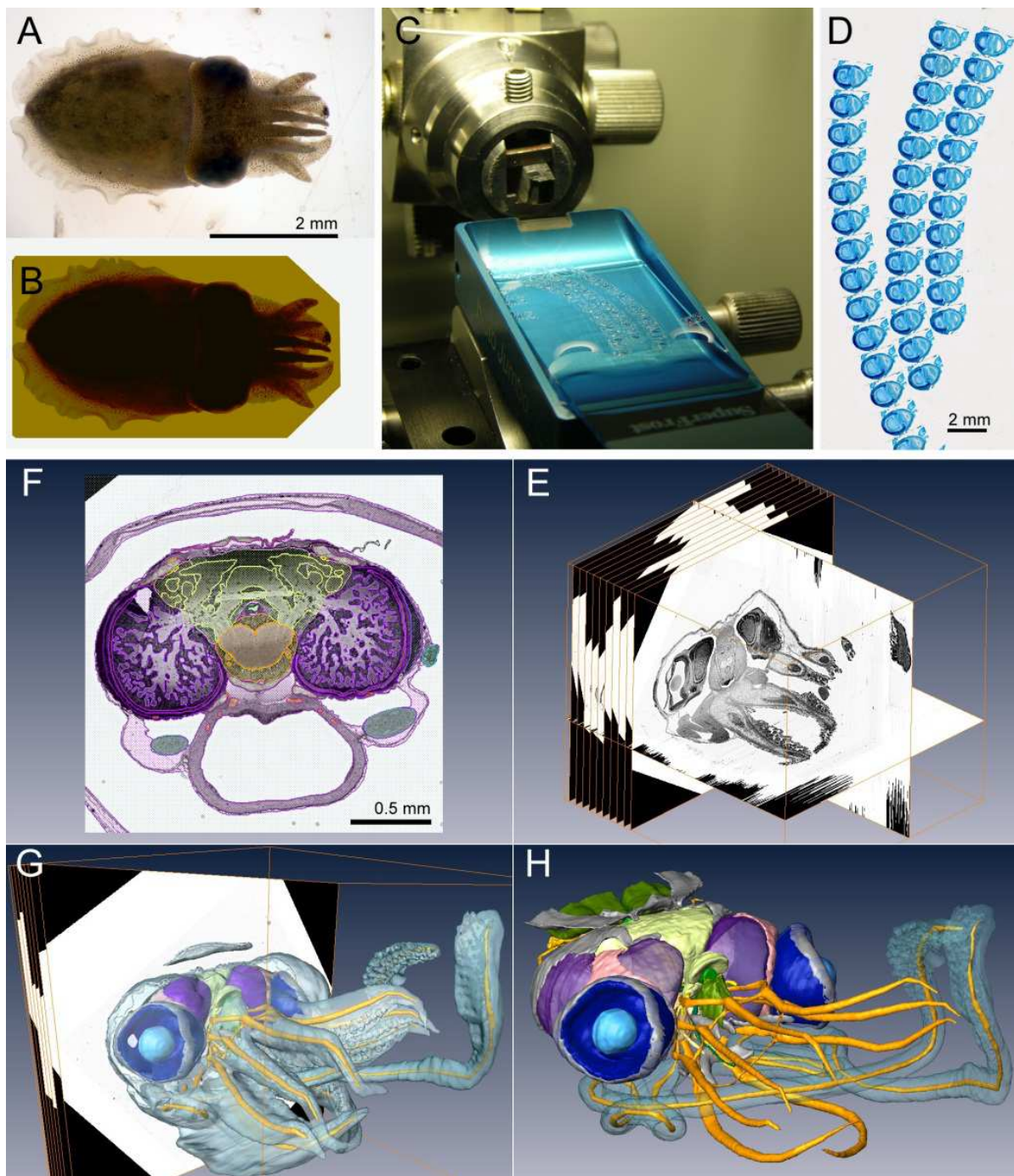
Fig. 2. From organisms to 3D-surface models (based on mechanical slices and light microscopy) **A** *Sepia* hatchling, chemically fixed. **B** *Sepia* hatchling contrasted with OsO$_4$ and embedded in epoxy resin. **C** Cutting the resin block in slice-ribbons with a diamond knife (1 µm thick). **D** Slice-ribbons stained with toluidine blue on a glass slide ready for light microscopy. **E** Stack of several hundred aligned digital images (= 3D-volume data) with orthogonal virtual reslicing planes. **F** Selected plane after manual segmentation of different tissue domains. **G** Surface rendering of the segmented domains emerging from the 3D-volume data. **H** 3D-surface model of the *Sepia* head in sub-µm resolution, allowing the interactive exploration of shape and constellation of all components, and morphometric analysis (B-D by H. Gensler; F-H by E. Scharpf).

indispensable for this task. To speed up the procedure and to bypass "bad" slices it is possible to interpolate the labels between two more or less distant planes.

2.1 Physical sectioning

Physical sectioning as maximally invasive "opening" of biological structures can be achieved, in principle, by two different approaches. Either the **slices** are collected, contrasted and imaged (commonly applied in transmission light or electron microscopy), or the slices are discarded and the **block-face** is imaged by reflected light microscopy or backscattering electron microscopy. Both approaches have advantages and disadvantages: imaging slices, as a rule, is more flexible concerning different staining protocols for biological tissues and tends to result in better 2D images (resolution and contrast) – imaging block faces, on the other hand, facilitates the alignment of neighbouring image planes for subsequent 3D-reconstruction (circumventing inevitable slice deformations) and avoids the loss of image planes owing to frazzled or furled slices. In the following these two approaches are explained exemplarily.

2.1.1 Imaging slices

There is quite a remarkable number of different possible method combinations for tissue fixation, embedding, cutting, staining and imaging slices. Object size and the desired contrast defines the embedding medium and as a consequence the cutting thickness and eventually the quality of 3D-reconstructions. In any case, one has to take care to obtain smooth, intact slices (single or ribbon) without losing slices or sequence information. In the process of image acquisition (flowchart step 8) one or several digital image stacks (e.g., different stainings on subsequent odd and even slices) are generated. The original specimen in the "refined" physical form of a section series may be stored in an archive or used for further investigations (e.g., cutting ultrathin sections from semithin sections). Four examples may give a glimpse into this broad method spectrum: **(1)** Vibratom sectioning of formalin- or paraformaldehyde-fixed soft tissue enclosed in agarose allows a section thickness down to 25 µm (kryosectioning even 5 – 10 µm) and is often used for fluorescence staining (e.g., lipophile neuron tracers, antibody staining, *in situ* hybridization); the vibratome section series can be imaged on a (fluorescence) stereomicroscope for 3D composition/analysis or single slices may be optically sectioned by CLSM (see section 3). **(2)** Paraffin- or historesin-sections of objects with diameters between 5 and 20 mm can be cut with steel knifes down to 5 µm thickness and subjected to any classical histochemical staining. After imaging with conventional light microscopy, 3D-rendering can be approached (flowchart steps 9 - 12), but artifacts from slice deformation can hamper digital post-processing. **(3)** Semithin section series (thickness 0.5 - 2 µm) cut with glass or diamond knifes from epoxy resin embedded specimens of less than 5 mm diameter provide the best quality for spatially accurate 3D-reconstructions (Fig. 2, see also Heß et al., 2008; Neusser et al., 2009). As a rule the slices are deformed insignificantly, ribboning is easy and minimal unevenness can be compensated by extended focal imaging light microscopy. The lateral resolution of the objective can be fully utilized and also z-resolution is outstanding. One shortcoming is the narrow palette of applicable staining reagents. **(4)** Ultrathin section series: as with semithin sections the resin-embedded material can be cut into so-called "ultrathin" sections of 40 - 100 nm. These flimsy sections are "fished" with grids (tiny metal washers with an central hole spanned by a ultrathin plastic film), contrasted with heavy metals (U, Pb) and imaged under the TEM. Yet, TEM-based 3D-reconstructions are possible (see e.g., Jörger et al., 2009).
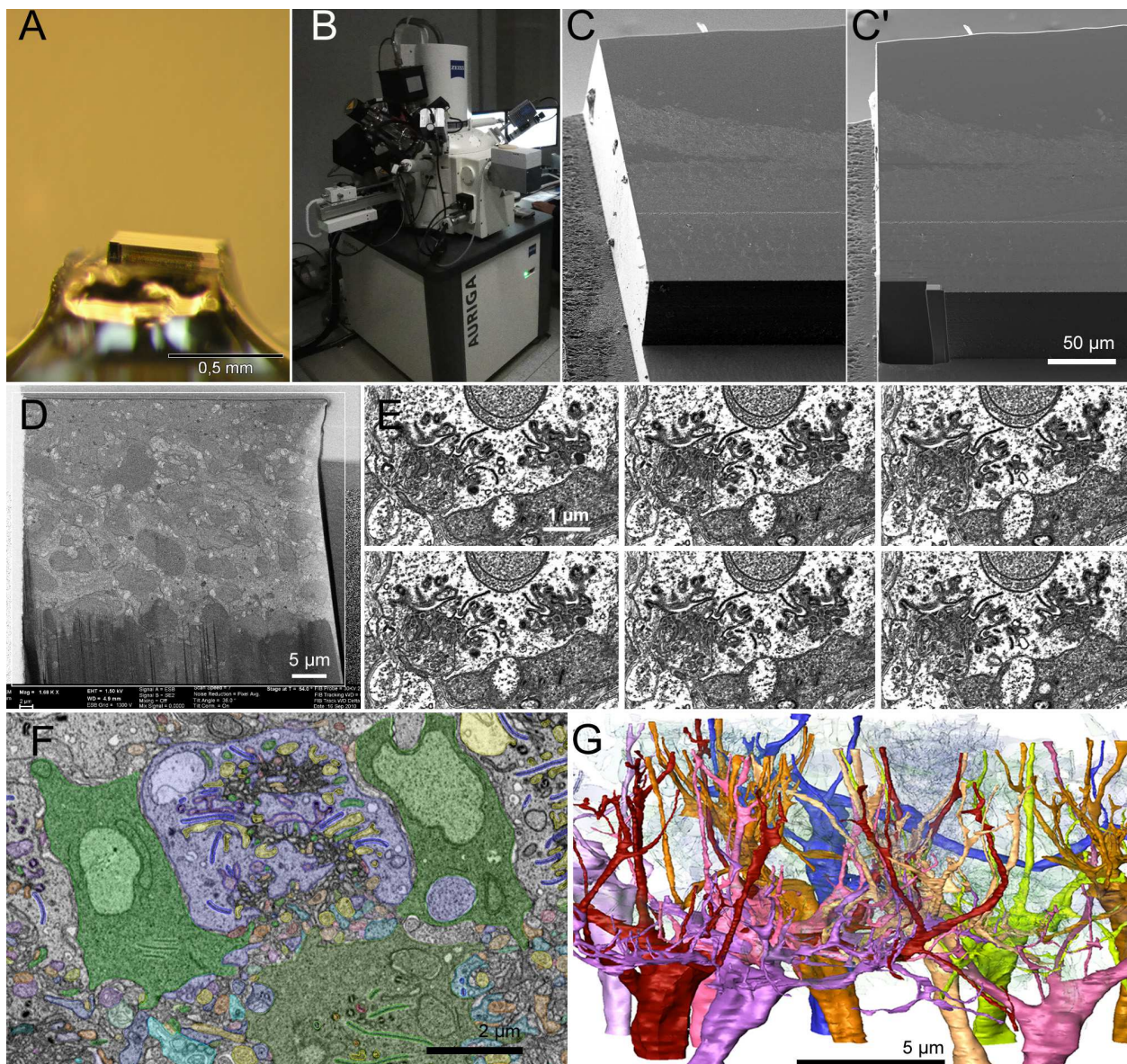
Fig. 3. Reconstructing neuronal nets in <10 nm isotropic resolution (FIB-FESEM-based) **A** Retina sample in epoxy resin trimmed by "mesa"-technique mounted on a minute specimen holder. **B** Zeiss "Auriga" cross beam workstation (FIB-FESEM = focused ion beam milling + field emission scanning electron microscope). **C** SEM image (secondary electron detection) of the mesa before ion beam milling. **C'** SEM picture of the same mesa after milling out a 35 x 15 x 65 μm^3 volume of interest. **D** SEM image (back scattering electron detection) of the block surface showing subcellular structures contrasted with OsO_4 and $[UO_2]^{2+}$. **E** Clipping of a FIB image series (showing the cable mess of retinal synapses) with a Z-spacing of 10 nm (columns) and 50 nm (rows). **F** Selected plane after manual segmentation of different neuronal branches (one colour for each cell, continuity retraceable only in 3D). **G** Surface rendering of a subpopulation of branching neurons in the volume of interest in 10 nm isotropic resolution (F, G by P. Koch).

2.1.2 Imaging block faces

On both sides of the size range of biological specimens designated for 3D-reconstruction, e.g. in centimeter- as well as in sub-micrometer dimensions, it can be advantageous (if not

the only practicable way) to image block faces instead of slices. **Histological** 10 μm slices of paraffin embedded specimens with a cutting area of several cm², e.g., are unstable and not manageable at all. A workaround is discarding the slice and carefully staining the block surface, before taking a macro image and scaling off the next slice. For **3D-electron microscopy**, on the other hand, with cutting areas of several μm² only, there is an alternative to TEM-imaging of ultrathin section series (problems see paragraph *alignment*, point 3), namely the "serial block face scanning electron microscopy" (SBF-SEM). Here, the specimen has to be contrasted with heavy metals (Os, U) before embedding in epoxy resin, thoroughly polymerized and carefully trimmed in mesa-shape with perfect object orientation. Then, the sample is cut within the vacuum chamber of a scanning electron microscope with field emission gun (FESEM) and backscattering electron (BE) detector. Two versions of SBF-SEM are currently available (with very few machines up to now): **(1)** the Gatan 3view, in which the sample is cut mechanically with a diamond knife in 25 - 50 nm layers and subsequently imaged with the electron beam using the BE detector. An advantage of this system is the large scanning area that can be achieved by stitching of adjacent fields-of-view without tradeoffs in resolution (max. ca. 20 nm/px). **(2)** crossbeam workstations (e.g., Zeiss Auriga) rest upon a focused (gallium) ion beam for milling off layers of down to less than 10 nm (!) and again BE detection with a scanning electron microscope (FIB-FESEM; see Fig. 3). With a FIB-FESEM an isotropic resolution of 10 nm voxels can be achieved, at the cost of a comparatively small field-of-view (e.g., 35 x 25 μm). SBF-SEM-based data allow for the precise 3D-reconstruction of neuronal networks with all synapses and connectivity rules in the VOI for the first time. Acquisition time (e.g., 75 hrs for 15 μm feed at 3 min/frame) and costs for gallium-emitter consumption are high. As a rule the data will exceed several GB, necessitating powerful imaging computers and graphic cards with sufficient RAM.

As mentioned above, the main drawbacks of physical slicing-based 3D-renderings are the time and effort needed for preparation, imaging, image post-processing and segmentation, as well as the complete destruction of the specimen. Ambitious efforts are undertaken to speed up the procedure, at least in parts. Automatic batch imaging of slice ribbons on several glass slides in combination with extended focal imaging is already available (e.g., Olympus dotSlide). Customized semi-automatic post-processing and 3D-segmentation tools (e.g., Jurrus et al., 2006; Yang & Choe, 2009) may facilitate the work flow in several fields of organismal biology. Additionally, in high-content applications such as 3D-EM analysis of neuronal networks, the KNOSSOS /RESCOPE methodology, in which many persons work together to segment structures in a single 3D-stack, is a promising approach for the future (Helmstaedter et al., 2011).

3. Confocal Laserscanning Microscopy (CLSM)

The accurate three-dimensional depiction of (selected) morphological features of given specimens has been possible for a long time by using serial sectioning techniques combined with light or electron microscopy (see above). However, the resulting obstacle, namely the significant time investment needed to yield these reconstructions, has significantly hampered large-scale comparative analyses. This was at least partly overcome with the introduction of confocal laserscanning microscopy (CLSM) to biological research, whereby pre-aligned optical stacks of digital images through a biological sample may be produced.

These stacks of individual, in-focus images may in a subsequent step be fused into projection images, thus rendering detailed, high resolution representations of the OOI throughout the depth of the sample. In addition, these stacks may be further processed by various imaging software packages to produce three-dimensional, volume and/or isosurface rendered reconstructions, as well as animations, that allow for viewing the given structures from various angles, thus facilitating detailed morphological analyses. This way, complex micro-anatomical structures, such as muscular or neural networks of microscopic animals, may be reconstructed within a few hours, a task that would take weeks or months to complete (if at all possible), if conventional sectioning techniques were to be applied (see Wanninger, 2007).

The breathtaking technological advances in laser technology, scan speed, temporal and spatial resolution of signal detection, *in silico* storage means, as well as software tools have undoubtedly fuelled the rapid establishment of confocal microscopy in the biological sciences since its commercial appearance some 30 years ago. As with numerous other biological research methodologies, the rapid establishment of CLSM as a routine research device after its demonstrated user friendliness in the mid-eighties was intimately linked to its usefulness in cell biological research (see also Amos & White, 2003; Pawley, 2006). The current state-of-the-art allows for high resolution depiction of cellular and subcellular structures unprecedented by light and fluorescence microscopical techniques before. As such, labelling of distinct proteins, cytoskeletal elements, chromosomes, and even single genes within an individual chromosome have rendered confocal applications highly interesting for basic research focusing on cellular ultrastructure, protein distribution, and the like.

3.1 Confocal applications on fixed samples

With the establishment of fluorescence staining procedures as routine laboratory techniques and the advancement and dramatic decrease in costs for computational power, confocal microscopy has significantly broadened organismal biological research. This has led to an explosion of morphological data on microscopic specimens, especially in zoological research (see, among others, Wanninger, 2009 for review). The huge success of confocal applications in this field of research is mainly due to the possibility of selective labelling of individual structures and organ systems such as muscles, neurons (including neuronal subsets such as transmitters and peptides), ciliary bands, or nephridia in entire organisms including individual developmental stages, which can subsequently be analysed using 3D-imaging software (Fig. 4). This has opened the door to explore numerous new pathways focusing on questions concerning the ontogeny and evolution of organ systems, unravelling developmental processes, and injecting entirely novel morphological datasets into issues concerning the interrelationships of animal phyla. Since the evolutionary driving force of character (state) selection takes place at all developmental stages, large-scale comparative, high resolution developmental analyses of organogenesis have generated important data on the microanatomy of developmental – often larval – stages that in such detail had not been available in the pre-confocal era (e.g., Brinkmann & Wanninger, 2008; Hessling, 2002; Hessling & Westheide, 2002; Kristof et al., 2008; Neves et al., 2009). As a most welcomed side effect, the sheer number of significant findings based on these advancements have catapulted evolutionary oriented organismal biological research – a field that often was
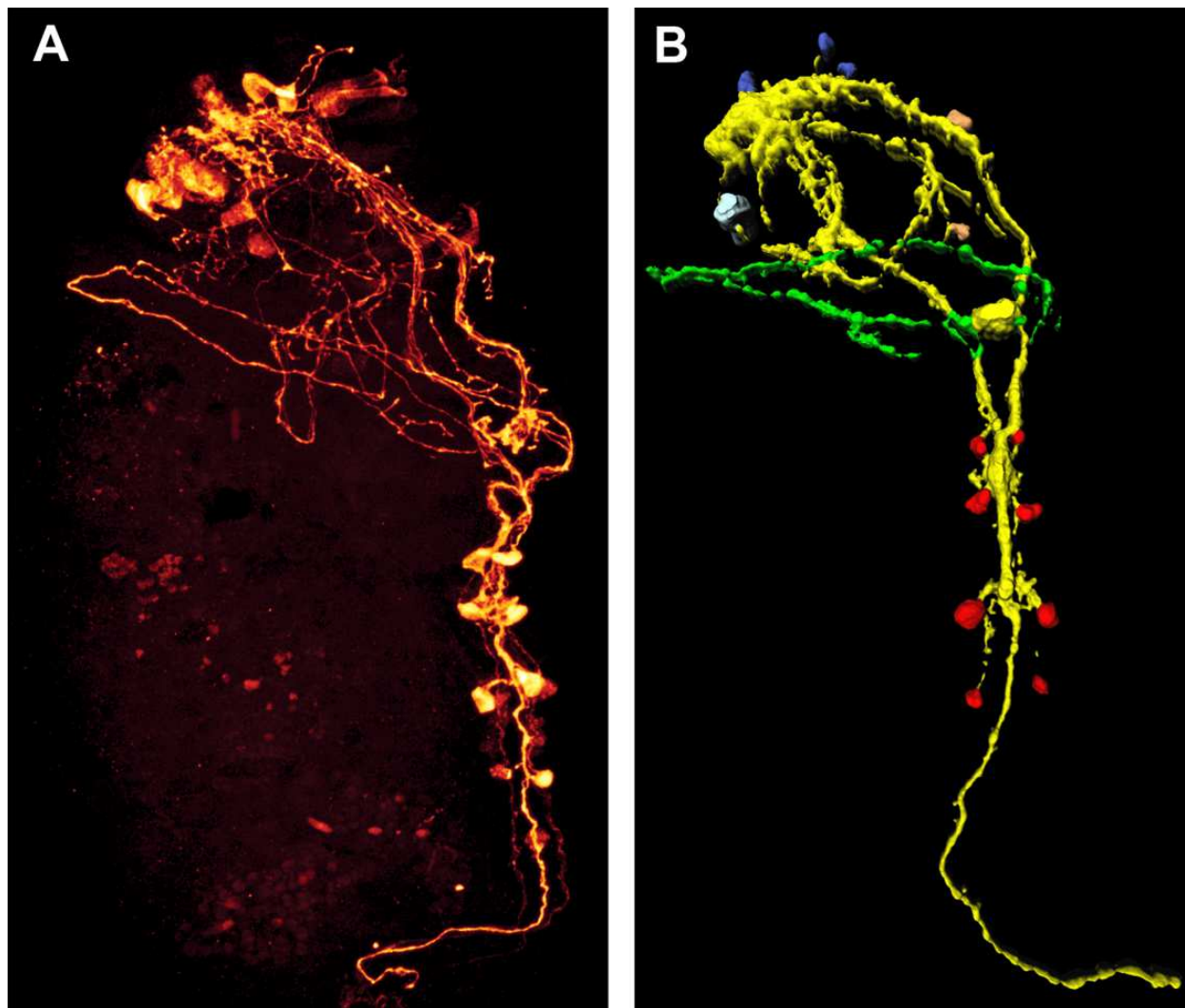
Fig. 4. Depiction of the serotonergic nervous system of a marine invertebrate worm.
A Maximum projection image of a confocal microscopy stack. **B** A stack similar to the one in A has been digitally modified with 3D-imaging software, whereby selective subsets of the immunoreactive parts have been highlighted by different colours. Approximate length of the individuals is 400 µm. (A, B by A. Kristof)

frowned upon as old fashioned and outdated – into the 21st century, and has led to an integration of morphological, developmental, and molecular approaches to solve evolutionary questions. As such, the detailed reconstruction of proliferating cells (by labelling of mitotic cells; Kristof et al., 2011) and gene activity (by *in situ* hybridization; Jékely & Arendt, 2007) using confocal imaging have and undoubtedly further will help to elucidate developmental processes in multicellular animals that entirely rely on fixed material. While classical single-photon confocal microscopy has routinely entered organismal biology, two- or multiphoton applications are yet not that widely spread. Using two- or multiple photon excitation allows for a far greater depth of penetration – up to 1000 µm sample thickness (Helmchen & Denk, 2005) – thus making multiple cellular layers within given, also living, tissues accessible to whole-mount confocal-type analysis. This is due to the fact that the strength of the fluorescence signal increases by the second power if two photons are excited (and is cubed in the case of triple-photon excitation, respectively),

thus allowing for significantly higher fluorescence signal than gained by single-photon excitation (Ustione & Piston, 2011). However, in order to generate multi-photon excitation, cost intensive pulsed laser beams need to be applied in order to reach the required photon density. In addition, resolution yielded with this technology is considerably lower than the one obtainable by single-photon confocal microscopy, thus hampering analyses that call for particularly high resolution images. Moreover, due to the higher laser power needed to penetrate the tissue, samples are prone to faster bleaching than in single-photon microscopy applications.

3.2 Live cell imaging

Combining the basic principles of fluorescence microscopy and the high resolution and fast scanning power of confocal laserscanning systems has led to numerous innovations that have enabled confocal recording of live tissue. Accordingly, it is now possible to observe cellular movements or subcellular activities (e.g., protein dynamics) in real time in all three spatial dimensions. Three of the most commonly used techniques in organismal research are thereby FRAP (fluorescence recovery after photobleaching), FLIM (fluorescence lifetime imaging microscopy) and FRET (fluorescence resonance energy transfer).

FRAP experiments involve controlled, irreversible bleaching of a specific area of interest in a living sample. Fluorescence in this region may be recovered by diffusion of fluorescing molecules from the neighbouring, non-bleached areas. This may be combined with GFP application, which allows for non-invasive, long-term studies of living cells and organisms. By measuring the diffusion time of the non-bleached molecules, the mobility rate of the molecule of interest may be inferred in addition to its mere localization. In addition, molecule-molecule interactions as well as signalling events may be followed using FRAP (Reits & Neefjes, 2001).

In FLIM measurements, the lifetime of a fluorescence signal is recorded. Fluorophores exhibit a defined lifetime, which is dependent on certain parameters, including concentrations of specific ions, proteins, oxygen, or the pH in its surrounding medium. Since these values directly correlate with the lifetime of the fluorescence of a given fluorophore, FLIM studies can be used to characterize and detect changes in the environment of living cells with respect to these parameters (Lakowicz et al., 1992). In order to achieve this, two laser pulses are necessary, one to excite the fluorophore at the start of the recording and a second one at the end of its lifetime. Accordingly, FLIM is typically used in combination with multiphoton microscopy, which delivers pulsed laser beams in the required intervals.

Recently, FRET has proven highly efficient to measure the interaction and co-localization of molecules in living systems at particular high temporal (on the nanosecond scale) and spatial (on angstrom level) resolution (Sekar & Periasamy, 2003). Thereby, energy is transferred from a donor to an acceptor fluorophore if their distance is less than 10 nm. While CFP/YFP and FITC/Rhodamine have traditionally been used as FRET pairs, these have nowadays widely been replaced by various GFPs. FRET is often used to measure cellular events such as calcium signalling and protein interactions, which may be particularly well resolved if combined with FLIM (Sekar & Periasamy, 2003). As with FLIM, FRET is often coupled to multiphoton microscopy using a white laser source which enables selection of the excitation wavelength that ideally matches the donor fluorophore.

Despite these obvious advantages, confocal laserscanning microscopy, as any other research tool, is limited by several parameters.

First, and most obvious, albeit a sophisticated device based on laser technology, its basic function still rests on the principles – and limitations - of conventional light microscopy (although these may partly be overcome by specialized application tools such as FRET, see above). Accordingly, if structures other than the very surface of a sample are to be scanned, the laser beam (excitation) as well as the resulting signal (emission) needs to penetrate the sample in order to yield a detectable signal. As a result, electron dense matter may significantly reduce scanning depth, which in many confocal applications generally is limited to the first upper 100 μm of a sample. As mentioned above, this may be increased by multiphoton setups, which penetrate deeper but come at a cost of lower resolution.

Second, and again in contrast to histological analyses, confocal data are typically generated for specifically stained structures (unless autofluorescence is recorded). Hence, and although multicolor staining procedures are often applied, one will never be able to reveal the structural organization of a sample in its entity. Thus, the relative placement or interaction of several, say, organ systems in an animal, are usually not inferable by confocal analysis alone. The otherwise desired high specificity of many agents, such as nucleic acid stains, phalloidin to label F-actin, antibodies against specific neurotransmitters or cytoskeletal components and the like may thus call for additional histology- or tomography-based investigations, especially if functional analyses are sought after.

Third, despite the high specificity of numerous markers, whole-mount preparations in particular are prone to high unspecific signal due to autofluorescence of various molecules at given excitation wavelengths. Chemically, this can be reduced by applying clearing media such as a mixture of benzyl benzoate and benzyl alcohol, which, however, might interfere with some stains (e.g., phalloidin). In confocal analyses, low signal-to-noise ratio might be enhanced by optimizing the excitation wavelengths for the respective fluorochromes by using a white laser which allows for selection of excitation wavelengths that perfectly match a given fluorophore. In addition to more efficient exploitation of the fluorophore, cross-excitation in multicolor experiments is reduced and, due to the lower excitation power needed, the viability of cells in *in vivo* investigations may be significantly increased. This is also true for certain novel, highly sensitive, low-noise detection systems based on single photon counting rather than secondary electron amplification by a photomultiplier tube (PMT) used in more standard confocal setups.

Overall, the strength of confocal applications in biological studies based on fixed samples lies in its high-throughput, high-resolution recording of selected, complex, yet minute microscopical structures. The resulting digital image stacks may subsequently be used for further 3D-processing employing, e.g., volume and surface rendering algorithms. In addition, quantitative studies including volumetrics and measurements of cellular contents can be obtained. In live (cell) imaging experiments, confocal microscopy allows for depictions of cellular processes, including molecular activity. The expected further technological improvement in the sensitivity of detection systems, scan speed and computational power should lead to even higher resolved recordings. It is expected that these further developments will in particular benefit experiments employing live confocal laserscanning imaging, thus moving towards highly resolved real-time recordings of biological processes in spatial resolution (e.g., depiction of organelles, bacteria, cells, organ systems or entire microscopic organisms moving and/or changing over time) – and therefore towards true, live, four-dimensional organismal microscopy.

4. Scanner-based non-invasive virtual sectioning techniques (CT/MRI)

At the end of the 19th century Wilhelm Conrad Roentgens` discovery of "a new kind of light" (Glasser, 1995) heralded a new era: "visualization into the body without painful and often life-threatening surgery" (Robb, 1982). Until now, roentgen radiation (X-ray) has been used as a non-invasive imaging method in diagnostics and was an important step towards the invention of X-ray computed tomography (CT). Another major breakthrough in medical radiology was the development of magnetic resonance imaging (MRI), which is based on the physical phenomenon that nuclei of atoms exposed to a magnetic field absorb and re-emit electromagnetic radiation. The foundation for both, CT and MRI was laid in 1973 and revolutionized non-invasive imaging while offering unprecedented *in vivo* insights into the human body. Increasing computational power set the stage for interactive 3D-models based on virtual sectioning and made medical imaging techniques even more attractive for the application in biological research. This development boosted life science research into a new era, thus enabling to look into an organism and navigating through all its anatomical features from every direction, which in turn provided new insights into morphological and functional coherences.

Both, CT and MRI, have several features in common in creating 3D-models from their recorded data. First, these data are obtained in a standard format for medical imaging (DICOM) that provides not only the image itself but also metadata (e.g., scanning parameters, patient information). Second, each single slice of the image stacks produced by CT and MRI scans consists of gray values that reflect tissue characteristics. Third, the CT and MRI data-sets does not only contain two-dimensional information of each single slice, it consists of three-dimensional pixels, so called "voxels" (= volume elements) which accurately reflect the volume information of a given OOI in isotropic resolution when using appropriate scanning parameters. The last fundamental step is image-based modeling of the data sets by the use of the appropriate computer software (see section 2). In contrast to medical applications, where in some cases automatic segmentation is available for precise 3D-modeling of a specific structure, CT and MRI scans of biological specimens often need intensive manual labour to extract the OOI from the surrounding tissue (see section 2, paragraph *segmentation*).

However, CT- and MRI-based methods not only pioneered medical diagnostics; they offer unique possibilities to unravel scientific questions beyond classical anatomical research in organismal biology. Especially anatomical investigations of rare museum species or species that are difficult to obtain renders scanner-based non-invasive virtual sectioning techniques a perfect tool in contrast to destructive dissections.

4.1 X-ray Computed Tomography (CT)

The invention of computer-based X-ray tomography by Hounsfield (1972, 1973) revolutionized diagnostics in medical radiology. In addition, this technique in combination with all advantages of subsequent 3D-imaging and the possibility of "true" real-time analyses have improved the capacity for innovation in Life Sciences (Schreurs et al., 2003). In general, the process of image acquisition from X-ray computed tomography (CT) is similar to classical radiology, whereby the OOI (e.g., the arm of a patient) is placed in the line between the X-ray source and the detector (e.g., film or digital detector). In this process, the different absorption patterns of the respective tissues are carried in the X-ray beam.

A major disadvantage of conventional radiology is summing up or superimposing of all points along the "single view" line, which leads to a blurry picture (Radon, 1917). Now, scanning around a transaxial plane allows to collect the beam only from a single point of the sample, preventing superposition (Robb, 1982). CT, therefore, produces virtual serial cross-sectional images of a given OOI. The obtained volume of data is a stack of slices, each slice being a digital two-dimensional grey value image. The given grey values basically represent the electron density of an object corresponding to the average attenuation of the X-ray beam which is quantified by the use of the Hounsfield scale (Kak & Slaney, 1988). Hounsfield Units (HU) range from - 1024 to + 3071 and are commonly set at 0 for water and - 1000 for air. Since humans are not capable of distinguishing over 4000 grey values, a process called "windowing" is applied to narrow the range of grey values of a given object for further image processing. A variety of software packages using sophisticated algorithms are available to subsequently reconstruct the scanned OOI in three dimensions. Given that for equivalent X-ray energy a denser structure will attenuate the beam more than a less dense structure, excellent 3D-reconstructions are produced by utilization of the natural contrast when a highly absorbing structure is surrounded by tissues with relatively weak absorbance (e.g., bones in contrast to soft tissues such as muscles; Boistel et al., 2011).

However, if the density of the different soft tissues are similar the use of appropriate contrasting agents is advisable. Conventional clinical CT scanners are designed for objects at the size and density of humans. In addition, non-lethal X-ray energies (~75 kV) are used in medical applications, which in turn foreclose a spatial resolution above 1 - 2 mm (Stuppy et al., 2003). However, with state-of-the-art helical CT scanners and higher X-ray doses, imaging of biological specimens with an isotropic resolution of 0.4 mm^3 (at 140 kV) is possible (Laforsch et al., 2008).

4.1.1 Organismal applications

The rapid advancement in tomographic imaging led to the development of scaled down clinical scanners (Mini-CT) which can provide a dataset of e.g. the torso of a mouse at an image resolution of 50 – 100 μm. Micro-CT scanners, on the other hand, image specimens at spatial resolutions from cellular (20 μm) down to subcellular dimensions (e.g., 1 μm; Dierolf et al., 2010) and fill the resolution-hiatus between optical microscope imaging and mini-CT imaging of intact volumes (Ketcham & Carlson, 2001; Ritman, 2004). However, micro-CT systems suffer from the drawback that high resolution can only be obtained for small samples with a maximum size of 5 – 30 mm (Metscher, 2009). Moreover, it often cannot be used *in vivo* because the applied X-ray doses are lethal (Stuppy et al., 2003). Next to medical applications, CT is often applied in biological studies examining functions of morphological structures or morphological differences between species. The physical properties of the tissue of interest reflected by X-ray attenuation renders mineralized structures such as bones or cartilage particularly suitable for CT (Kruszyński et al., 2007). Hence, studies using CT-based 3D-reconstructions have focused on the depiction of coarse and subtle details of the skeleton in mammals (Marino et al., 2003), fish (Claeson et al., 2007), amphibians (Maddin, 2011) or reptiles (Maisano & Rieppel, 2007). Nevertheless, CT can also be applied to analyse soft tissues. For instance, Wirkner & Prendini (2007) examined the morphology of the hemolymph vascular system in scorpions using micro-CT and 3D-reconstruction.

A further application of CT is centred in Palaeobiology to study fossils in a non-destructive way (Macrini et al., 2007; Rogers, 1999; Vasquez et al., 2008). This facilitates to reveal the nature of the fauna and flora of past ages and therefore boost evolutionary studies.

To illustrate that CT-derived 3D-models offer unique possibilities to unravel scientific questions beyond classical anatomical research, here an example from coral reef ecology will be presented:
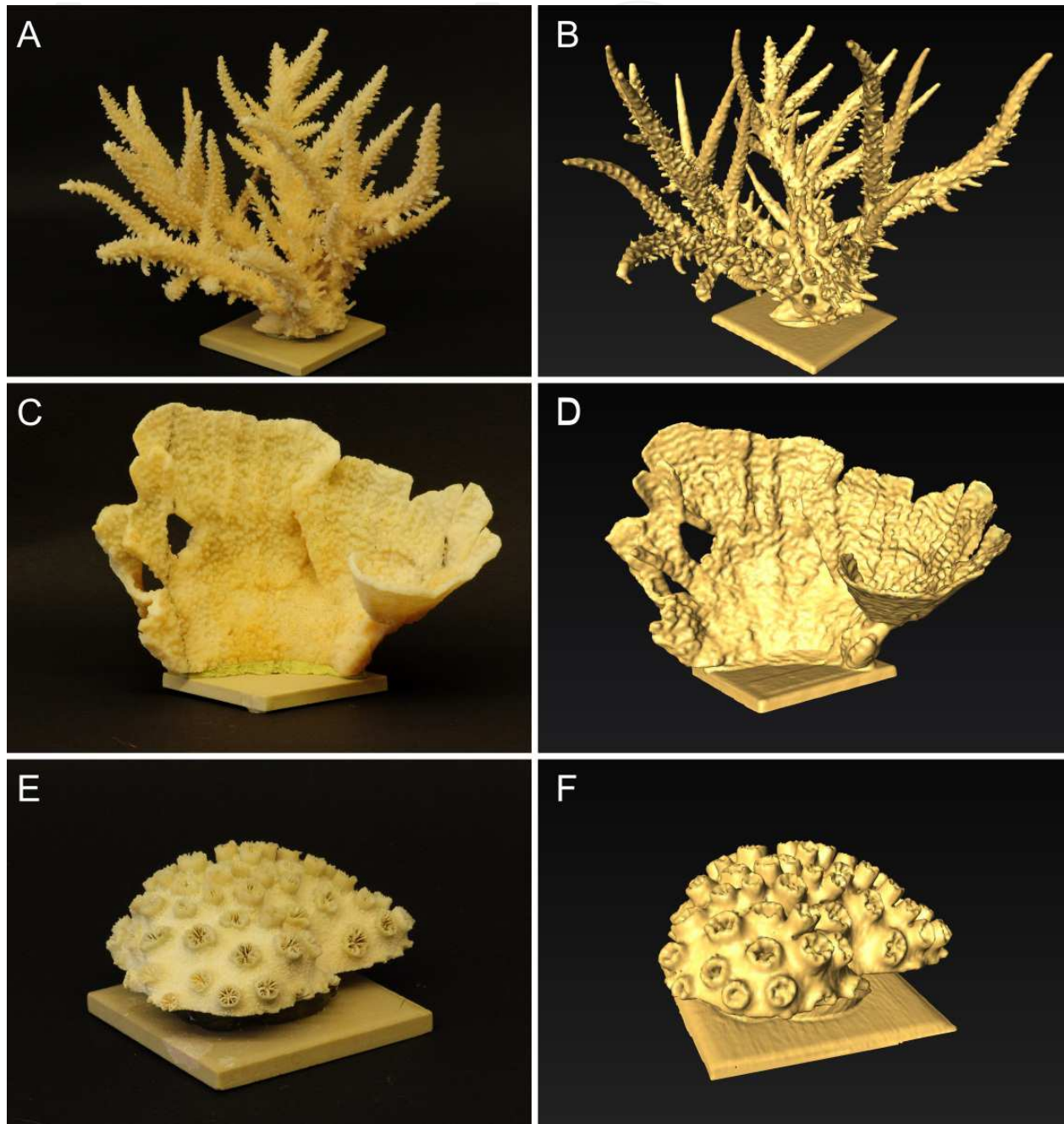

Fig. 5. Coral growth forms imaged with X-ray computed tomography and 3D-reconstruction. Photographies of different coral skeletons (left column) and associated 3D-models based on X-ray computed tomography (right column). **A** & **B** Branching staghorn coral (*Acropora sp*.). **C** & **D** Encrusting coral (*Montipora foliosa*). **E** & **F** Massive-growing coral with large polyps (*Galaxea fascicularis)*.

Coral reefs are among the most diverse and productive ecosystems on Earth. Corals occur in a variety of growth forms, and there is strong variation in coral shape even within a single species. Quantifying this variation is relevant for a wide range of ecological studies. Moreover, the question of how to determine the surface area in this phenotypically plastic organism has been of considerable interest in several studies in coral reef science. For instance, the surface area of corals serves as an important reference parameter for the standardization of metabolic processes such as photosynthesis or respiration. Hence, a variety of methodologies have been introduced and applied to determine the morphology, volume and surface area of corals, however, all of them being destructive.

Given the fact that the attenuation of the X-ray beam in calcium carbonate differs extremely from the surrounding medium (e.g., seawater), the shape of the coral skeleton can be easily extracted during image processing with the suitable software (see section 2, paragraph *segmentation*) to generate a virtual clone of the respective coral colony (Kaandorp et al., 2005). Since the calcified skeleton resembles the surface area of the very thin tissue layer of the coral, Laforsch et al. (2008) applied conventional medical CT in living coral colonies, thus enabling highly accurate surface area measurements from the isosurface of the volume data in a non-destructive way (Fig. 5).

A limitation of CT application arises from the fact that it is hardly applicable in the field, although portable CT scanners are already available. Another limitation of CT is the restriction to measurements of the skeleton topography only, while for example coral tissue components remain undetected. To achieve a higher spatial resolution, which in turn enables imaging of delicate details, greater X-ray fluxes are required, hence, evoking an inherent trade-off between image quality and tissue damage (Boistel et al., 2011).

However, sophisticated state of the art technologies in CT in combination with classical methods will enable scientists to improve their knowledge on ecosystem function. Moreover, the breathtaking advancement in CT technology sets the stage for unimagined new possibilities in life science research. Newly developed synchrotron scanners offer a significantly higher resolution, a better signal-to-noise-ratio, and the potential for quantitative reconstructions (Betz et al. 2007) with a resolution down to about 60 - 90 nm (Baruchel et al. 2008).

4.2 Magnetic Resonance Imaging (MRI)

Lauterbur (1973) produced the first 2D-image using MRI-technique depicting two H_2O-filled glass capillaries in a D_2O environment. He paved the way for MRI-based applications in medicine, while today MRI body scanners are standard diagnostic tools in almost every hospital of the developed nations (Glover & Mansfield, 2002). Clinical research on human diseases using small mammals as model systems strongly favoured the invention of small animal MRI and magnetic resonance microscopy (MRM, µMRI, micro-MRI; Benveniste & Blackband, 2002). The difference of MRM to conventional MRI is that the achieved resolution is usually lower than 100 µm and that micro-MRI chambers are typically small (1 cm^3). The higher resolution in micro-MRI is predominantly produced by stronger field strengths of the magnets (e.g., up to 21 Tesla (T) for micro-MRI compared to 1-3 T for conventional MRI).

MRI technique is based physically on the principle of nuclear magnetic resonance (NMR). Since protons and neutrons in a nucleus own a magnetic moment (spin), they behave like a tiny magnet. Exposed to a magnetic field these nuclear magnetic moments align to form a

so-called longitudinal magnetization parallel to the external magnetic field. By applying radio-frequency (RF) pulses this longitudinal magnetization is tilted into the plane perpendicular to the magnetic field, forming the so-called transverse magnetization. The latter rotates about the direction of the magnetic field (the so-called precessional motion) and – thus being a temporally varying magnetic field itself – induces an alternating electric current in a receiver coil. This current, the so-called MR-signal, is translated into grey value image stacks containing the accurate volume information. Different grey values reflect the varying properties of water and lipid protons in different tissue types. These properties are mainly the proton density and the so-called relaxation times T1 and T2, which characterize the return of the proton magnetization system back to its equilibrium state after having been disturbed by the RF pulse. Crucial for the discrimination of different tissue types is their difference in grey values, the so-called contrast, which should be maximized for computerized 3D-reconstruction (see also below for the role of image quality). Different MR image contrasts are mainly achieved by varying scanning parameters such as repetition time, echo time or flip angle in order to emphasize one or more of the tissue parameters mentioned above. One then speaks of "proton density weighted", "T1 weighted" or "T2 weighted" images. In addition, mixed forms of image contrast can be achieved by applying appropriate combinations of scanning parameters.

Other crucial parameters for 3D-reconstruction are spatial resolution and image quality. Concerning resolution, the smaller the OOI (e.g., organs of an animal) the higher the spatial resolution of the images has to be in order to minimize the uncertainty when it is about to obtain quantitative data.

Like any other measurable quantity, the signal intensities or grey values of an MR image are not exact but can only be determined within certain error bounds, the so-called image noise. Image quality is usually quantified as so-called „signal-to-noise" ratio (SNR, e.g., grey value divided by the noise figure), whereas it is the so-called '"contrast-to-noise" ratio (CNR) which determines how well two adjacent organs of different tissue type can be discriminated, and is calculated by simply subtracting the signal-to-noise ratios of the tissues under consideration.

Finally, the quantities spatial resolution and SNR cannot be optimized independently from a third important parameter, the net scan duration. The three parameters SNR, the volume measure V of the voxel and the net scan duration T are interlinked via the equation (with 'α' indicating proportionality):

$$SNR \propto V \cdot \sqrt{T}$$

Thus, if one needs high spatial resolution (small V) and sufficient SNR for 3D-reconstruction of adjacent objects (large CNR) one has to choose a long scan time T. Or, to put it in more physical terms, as the MR signal intensity of a voxel is directly proportional to the number of contributing spins and thus proportional to the volume of the voxel, the weaker signal from a smaller voxel has to be compensated by averaging it over a longer period of time to reduce the root-mean-square deviation of the statistical fluctuations of the signal (for further readings see Vlaardingerbroek & Den Boer, 2003).

4.2.1 Organismal applications

The centrepiece of a conventional MRI scanner is a magnet with a bore diameter that provides enough space to scan a human body. The opening of the magnet bore and the achievable

resolution is also what limits the application of conventional MRI to certain biological issues. However, after Aguayo et al. (1986) had published the first MRI image of a toad egg, MRI-based methods became a promising achievement in organismal biology. For microscopic objects, where high resolutions are indispensible, micro-MRI is used, for bigger organisms and where resolutions of less than 100 µm are not required, conventional clinical MRI is applicable. Hence, 3D-models of virtual MRI sections are nowadays important tools in biological disciplines ranging from developmental biology to evolution and ecology, but also increasingly in genetics, physiology and neurobiology. They frequently are applied when it is about to gain a deeper look into preserved or living organisms without being invasive or destructive. A frequent application of MRI is centred in taxonomy. For instance, Ziegler et al. (2008) used micro-MRI-based 3D-models for the systematic comparison of sea urchins. The authors focused on selected soft tissue characteristics to analyse phylogenetic relationships, which would have not been detected by the use of traditional techniques (see section 2).

In line with this, it used to be a frontier for developmental biologists to follow the development of internal soft structures in one and the same individual over time. Traditionally, invasive histological sections that provide high spatial resolution were applied, but with the limitation that tissue preparation may cause artefacts that hamper the interpretation of the data. Furthermore, series of animals preserved in different developmental stages could only provide snapshots of the entire ontogeny. In recent years, researchers have overcome this restriction by the application of MRI-based methods. For instance, Bain et al. (2007) accomplished, by the use of MRI, to display the entire development of a chicken embryo *in ovo* for the first time. In addition, MRI and micro-MRI-based studies followed by 3D-modeling offer the unique possibility to depict intricate morphologies in anatomical atlases within decent time (e.g., Ruffins et al., 2007). Such 3D-atlases not only foster studies on pure anatomical issues, they may provide also an outstanding tool to display molecular pathways and gene expression patterns (Louie et al., 2000).

The rapid advancement of MRI technologies and applications even fuels studies on interrelationships between organisms. Quantitative data derived from 3D-models such as volume and surface areas are often needed in ecological studies and non-destructive MRI-based techniques offer plenty of possibilities to achieve these data *in vivo*. To illustrate the use of MRI derived 3D-models in ecology, an example from the marine system will be presented in the following:

The crown-of-thorns starfish *Acanthaster planci* is one of the most studied organisms in coral reef ecology (Moran, 1986). Due to population explosions they cause fatal damage to coral reefs in the Indo-Pacific region and the Red Sea. The reasons for the emergence of these population explosions are still subject to speculations; therefore, fundamental research on this animal has been a major topic in reef research for many decades. As population explosions, so called outbreaks, are by nature closely related to spawning events, it is indispensable to assess the spawning season of *A. planci*. Therefore, the reproductive status of its gonads has to be quantified, which is done by calculating so-called gonad indices. In this process the size, weight or volume of the organ is determined and set into relation to the respective parameter of the starfish. The bigger the index is, the closer the starfish is to its spawning season. Classical methods to estimate the size of these organs are lethal to the starfish, since *A. planci* has to be dissected for weighting their mass. A novel method has recently been established by Sigl & Imhof (unpublished data) to accurately calculate the volume of the inner organs of *A. planci in vivo*. The MRI-based method enables to determine
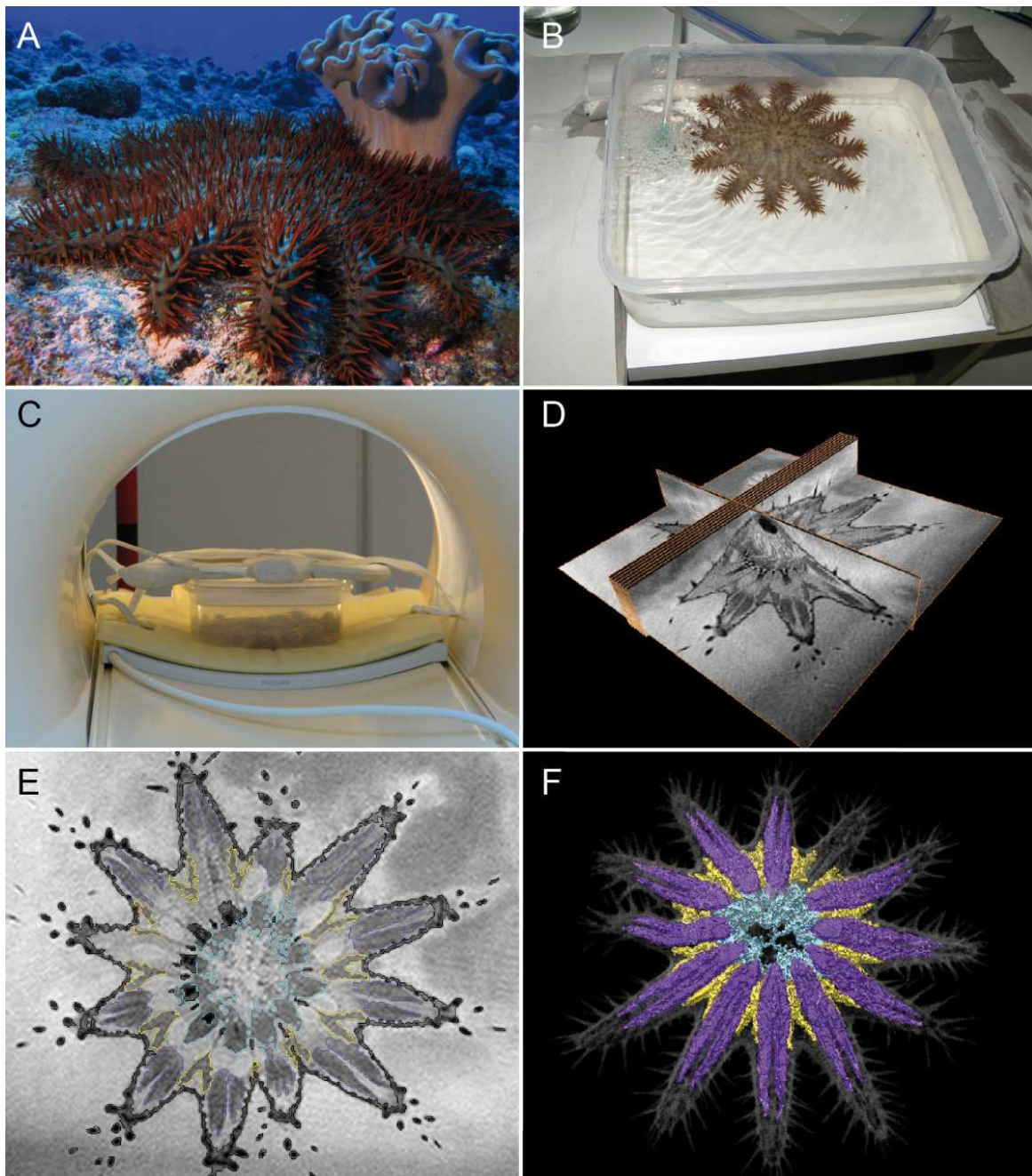
Fig. 6. From organisms to 3D-models, based on magnetic resonance imaging (MRI).
A *Acanthaster planci* individual on the reef. **B** Relaxed *A. planci* individual in a plastic box prepared for scanning using MRI. **C** Plastic box with *A. planci* in the MRI chamber with receiver coil on top. **D** Image stack obtained from MRI scan (3D volume data) with virtual planes (only a few planes are pictured). **E** Horizontal cross-sectional image (MRI-scan) of *A. planci* with outlined (segmentated) organs. **F** 3D-model (volume-rendered) of the starfish and its inner organs (grey: body wall/skeletal elements; purple: pyloric caeca; yellow: gonads; cyan: cardiac stomach).

the indices for a given individual over time, which is a major advantage, since individual differences do not bias the obtained data. Using conventional clinical MRI the organs of *A. planci* can be depicted. The obtained volume data set is subsequently used to render a

3D-model of these organs (Fig. 6). With the aid of these 3D-models and the known size of each voxel it is possible to accurately calculate the volume of these organs, and therefore also to detect size changes, which are a reliable indicator to assess the spawning season.

4.3 Juxtaposition of MRI and CT

Organismal biology benefits significantly from both, virtual sectioning methods, MRI and CT, which offer 3D-data sets in a, at first glance, non-invasive way. Especially for rare specimens, sensitive samples as well as for repeated measures, both techniques seem perfectly suitable.

However, CT uses ionizing radiation and there is direct evidence from epidemiologic studies that the radiation dose of a single common CT-study leads to an increased cancer risk for human adults (Brenner & Hall, 2007). Accordingly, in terms of *in vivo* studies in biological systems, CT clearly is rather non-destructive than non-invasive. Nevertheless, compared to MRI, the scanning times of CT are very low, thus enabling imaging of living organisms without the need of long term anaesthetics which may bias experimental conditions.
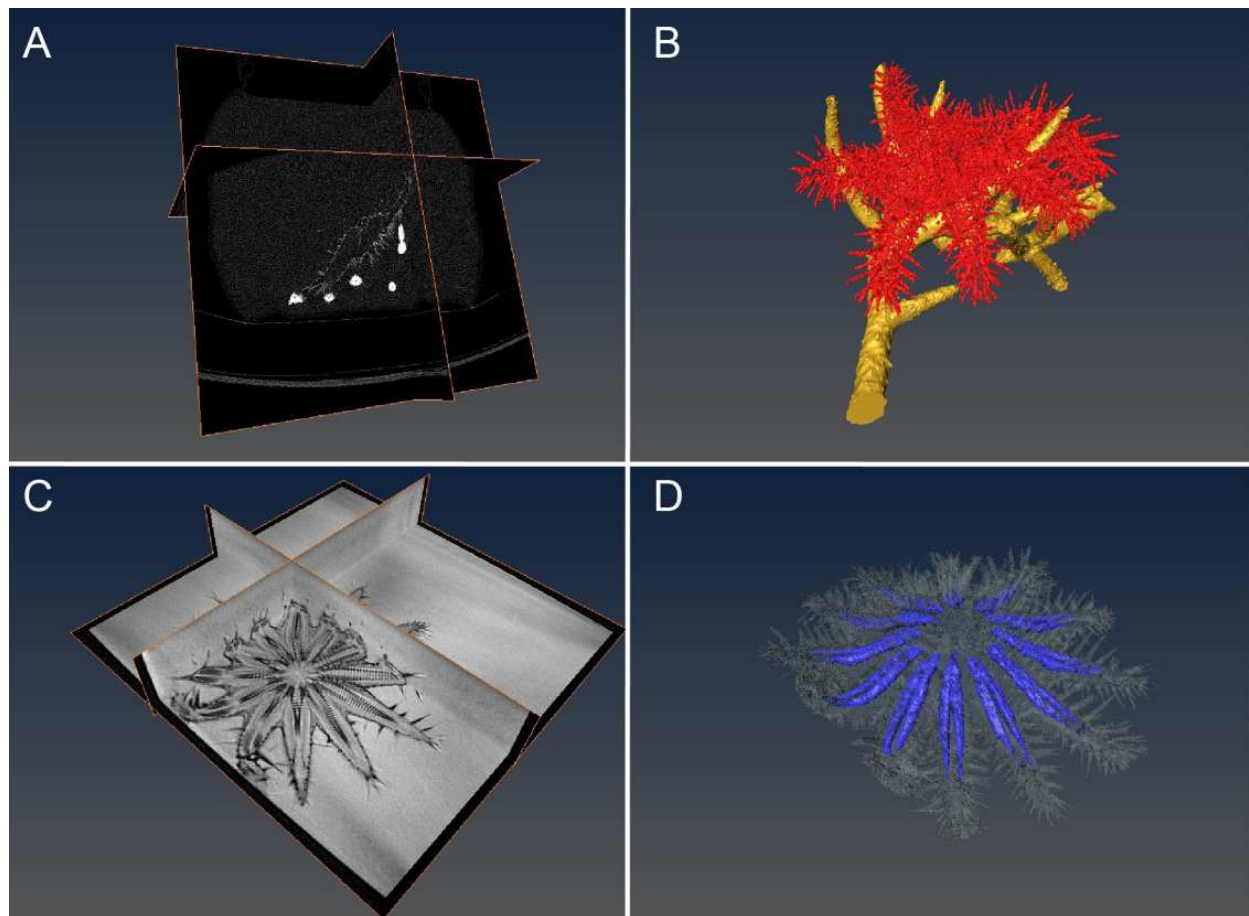

Fig. 7. Comparison of CT & MRI gained data illustrating functional limits of both techniques. **A** Image stack obtained from CT scan (3D volume data) with virtual planes (only a few planes are pictured) of a living *A. planci* individual crawling on a piece of coral. **B** 3D-rendered model of these CT data imaging all calcareous structures (red: starfish; golden: coral). **C** Image stack obtained from MRI scan (3D volume data) with virtual planes (only a few planes are pictured) of a living *A. planci* (anesthetized). **D** 3D-rendered model of these MRI data imaging outer morphology (transparent) and an internal organ (pyloric caeca, blue).

In marked contrast to CT, MRI is based on the detection of proton densities and is therefore advantageous when examining soft tissues. Hence, MRI is supposed to be "a real non-invasive" method, although effects of strong magnetic fields on organisms are by now not fully understood. Further, it offers the possibility for diffusion studies of fluids and the quantification of fluid flows (Walter et al., 2010). In addition, calcified structures can be depicted, but are likely to produce artefacts (Vlaardingerbroek & Den Boer, 2003). These can be suppressed by using certain scanning sequences, however resulting in lower signal-to-noise ratios or longer scanning times. Both methods have their strengths and weaknesses, thus, being mindful of the experimental design and the scientific question, the adequate technique can be selected.

Given that CT and MRI are complementary to each other in a way that CT can produce a distinct contour of mineralized structures such as bones, and MRI can show the adjacent soft tissue (Fig. 7), the development of fusion technologies to depict both data sets in a single 3D-reconstruction are well underway (e.g., Wong and Bishop, 2008). Recent technological progress has led to the development of combined Positron Emission Tomography (PET) and CT or MRI scanners in a single device, providing simultaneous information on metabolic pathways respectively anatomical characteristics in high spatial resolution. Hence, further technical advancement in this field will significantly improve non-destructive 3D live imaging in organismal biology.

5. Conclusion

Although digital imaging and computerized 3D-modeling is a rapidly advancing and promising technique in organismal biology, the interpretation of the visualized data should be handled with care, since the resolution of each acquisition technique differs and therefore relevant details of some biological structures will not be displayed in its entity or may even be entirely lacking. In addition, it has to be considered that there are many pitfalls while converting or even viewing the gathered data, as for example the absolute intensity information is lost in most image viewers, since they rescale the image to cover the maximal dynamic range (Walter et al., 2010).

Nevertheless, if the researcher is aware of those drawbacks, 3D-modeling opens new avenues for a variety of research areas in biology such as functional morphology or evolutionary developmental biology. It may even foster environmental sciences as it allows for accurate biomass calculations or the establishment of taxonomic 3D-libraries in biodiversity research. The latter will enable a high throughout identification, since the 3D-nature of organisms is crucial for a reliable morphological identification (Boistel et al., 2011).

In addition to the described digital imaging techniques there are numerous other 3D-based methods that become increasingly important in biological research. For example, using 3D-ultrasound microscopy at 1,2 Ghz, Laforsch et al. (2004) showed that small planktonic organisms strengthen their armour in the presence of an invertebrate predator and thereby uncovered a hidden inducible morphological defence. This study distinctly shows that imaging techniques are not only crucial to display morphologies in detail but also give striking insights into the ecology and evolution of these organisms.

Hence, the application of further improving techniques such as Atomic Force Microscopy (AFM), Optical Coherence Tomography (OCT) or superresolution light microscopy (e.g., 3D-SIM) are promising tools in organismal biology. With the development of even better

imaging techniques and the still increasing computational power, at continuously decreasing acquisition costs, 3D-models will revolutionize several fields in biological science. The current possibility to implement and present interactive 3D-models and animations in online publications and scientific databases offer the unique possibility to share a complete dataset with the scientific community (e.g., https://www.morphdbase.de, http://www.digimorph.org). This enables to interact with the discovered or reviewed issues not only in 2D but rather in 3D/4D. Overall, next to understanding delicate and complex biological structures, 3D-imaging is an outstanding tool to discover and document biological processes down to the molecular level in real-time with precise spatial information.

6. References

Aguayo J. B., Blackband S. J., Schoeniger J., Mattingly M. a. & Hintermann M. (1986). Nuclear magnetic resonance imaging of a single cell. *Nature,* Vol. 322, pp. 190-191

Amos W. & White J. (2003). How the confocal laser scanning microscope entered biological research. *Biology of the Cell,* Vol. 95, No. 6, pp. 335-342, ISSN: 0248-4900

Bain M. M., Fagan A. J., Mullin J. M., McNaught I., McLean J. & Condon B. (2007). Noninvasive monitoring of chick development in ovo using a 7T MRI system from day 12 of incubation through to hatching. *Journal of magnetic resonance imaging,* Vol. 26, pp. 198-201

Bardell D. (1983). The first record of microscopic observations. *BioScience,* Vol. 33, No. 1, pp. 36-38, ISSN: 00063568

Benveniste H. & Blackband S. (2002). MR microscopy and high resolution small animal MRI: applications in neuroscience research. *Progress in Neurobiology,* Vol. 67, pp. 393-420

Boistel R., Swoger J., Kržič U., Fernandez V., Gillet B. & Reynaud E. G. (2011). The future of three-dimensional microscopic imaging in marine biology. *Marine Ecology,* pp. 1-15, ISSN: 1439-0485

Brenner D. J. & Hall E. J. (2007). Computed Tomography — An increasing source of radiation exposure. *New England Journal of Medicine,* Vol. 357, No. 22, pp. 2277-2284, ISSN: 0028-4793

Brinkmann N. & Wanninger A. (2008). Larval neurogenesis in *Sabellaria alveolata* reveals plasticity in polychaete neural patterning. *Evolution & Development,* Vol. 10, No. 5, pp. 606-618, ISSN: 1525-142X

Claeson K. M., Bemis W. E. & Hagadorn J. W. (2007). New interpretations of the skull of a primitive bony fish *Erpetoichthys calabaricus* (Actinopterygii: Cladistia). *Journal of Morphology,* Vol. 268, No. 11, pp. 1021-1039, ISSN: 1097-4687

Dierolf M., Menzel A., Thibault P., Schneider P., Kewish C. M., Wepf R., Bunk O. & Pfeiffer F. (2010). Ptychographic X-ray computed tomography at the nanoscale. *Nature,* Vol. 467, No. 7314, pp. 436-439, ISSN: 0028-0836

Ellis J. & Solander D. (1786). *The natural history of many curious and uncommon zoophytes collected from various parts of the globe*. Benjamin and Son Horace's Head, Fleet Street

Glasser O. (1995). W. C. Roentgen and the discovery of the Roentgen rays. *American journal of roentgenology,* Vol. 165, pp. 1033-1040

Glover P. & Mansfield S. P. (2002). Limits to magnetic resonance microscopy. *Reports on Progress in Physics,* Vol. 65, pp. 1489-1511

Helmchen F. & Denk W. (2005). Deep tissue two-photon microscopy. *Nature Methods,* Vol. 2, No. 12, pp. 932-940

Helmstaedter M., Briggman K. L. & Denk W. (2011). High-accuracy neurite reconstruction for high-throughput neuroanatomy. *Nature Neuroscience,* Vol. 14, No. 8, pp. 1081-1088, ISSN: 1097-6256

Heß M., Beck F., Gensler H., Kano Y., Kiel S. & Haszprunar G. (2008). Microanatomy, shell structre and molecular phylogeny of *Leptogyra, Xyleptogyra and Leptogyropsis* (Gastropoda: Neomphalida: Melanodrymiidae) from sunken wood. *Journal of Molluscan Studies,* Vol. 74, No. 4, pp. 383-401

Hessling R. (2002). Metameric organisation of the nervous system in developmental stages of *Urechis caupo*; (Echiura) and its phylogenetic implications. *Zoomorphology,* Vol. 121, No. 4, pp. 221-234, ISSN: 0720-213X

Hessling R. & Westheide W. (2002). Are Echiura derived from a segmented ancestor? Immunohistochemical analysis of the nervous system in developmental stages of *Bonellia viridis. Journal of Morphology,* No. 252, pp. 100-113

Hounsfield G. N. (1972). *A method of and apparatus for examination of a body by radiation such as X-ray or gammaradiation*. British patent office, No. 12839153. Great Britain.

Hounsfield G. N. (1973). Computerized transverse axial scanning (Tomography). I. Description of system. *British Journal of Radiology,* Vol. 46, No. 552, pp. 1016-1022, ISSN: 0007-1285

Jansen J. F. A., Backes W. H., Nicolay K. & Kooi M. E. (2006). 1H MR spectroscopy of the brain: absolute quantification of metabolites. *Radiology,* Vol. 240, pp. 318-332, ISSN: 2402050314

Jékely G. & Arendt D. (2007). Cellular resolution expression profiling using confocal detection of NBT/BCIP precipitate by reflection microscopy. *BioTechniques,* Vol. 42, pp. 751-755

Jörger K., Heß M., Neusser T. & Schrödl M. (2009). Sex in the beach: spermatophores, dermal insemination and 3D sperm ultrastructure of the aphallic mesopsammic *Pontohedyle milaschewitchii* (Acochlidia, Opisthobranchia, Gastropoda) *Marine Biology,* Vol. 156, No. 6, pp. 1159-1170, ISSN: 0025-3162

Jurrus E., Tasdizen T., Koshevoym P., Fletcher P. T., Hardy M., Chien C.-B., Denk W. & Whitaker R. (2006). Axon tracking in serial block-face scanning electron microscopy. *Proceedings of Workshop on microscopic image analysis with applications in biology*, October 2006

Kaandorp J. A., Sloot P. M. A., Merks R. M. H., Bak R. P. M., Vermeij M. J. A. & Maier C. (2005). Morphogenesis of the branching reef coral *Madracis mirabilis. Proceedings of the Royal Society B: Biological Sciences,* Vol. 272, No. 1559, pp. 127-133

Kak A. C. & Slaney M. (1988). *Principles of computerized tomographic imaging*. IEEE Service Center, Piscataway, NJ, USA

Ketcham R. A. & Carlson W. D. (2001). Acquisition, optimization and interpretation of X-ray computed tomographic imagery: appliciations to the geosciences. *Computers & Geosciences,* Vol. 27, No. 4, pp. 381-400, ISSN: 0098-3004

Kristof A., Wollesen T., Maiorova A. S. & Wanninger A. (2011). Cellular and muscular growth patterns during sipunculan development. *Journal of Experimental Zoology Part B: Molecular and Developmental Evolution,* Vol. 316B, No. 3, pp. 227-240, ISSN: 1552-5015

Kristof A., Wollesen T. & Wanninger A. (2008). Segmental mode of neural patterning in Sipuncula. *Current Biology,* Vol. 18, No. 15, pp. 1129-1132, ISSN: 0960-9822

Kruszyński K., Kaandorp J. & van Liere R. (2007). A computational method for quantifying morphological variation in scleractinian corals. *Coral Reefs,* Vol. 26, No. 4, pp. 831-840, ISSN: 0722-4028

Laforsch C., Ngwa W., Grill W. & Tollrian R. (2004). An acoustic microscopy technique reveals hidden morphological defences in Daphnia. *Proceedings of the National Academy of Sciences of the United States of America,* Vol. 101, No. 45, pp. 15911-15914

Laforsch C., Wild C., Glaser C. & Niggl W. (2008). A precise and non-destructive method to calculate surface area in living sclerectinian corals using X-Ray computed tomography and 3D modeling. *Coral Reefs,* Vol. 27, pp. 811-820

Lakowicz J. R., Szmacinski H., Nowaczyk K., Berndt K. W. & Johnson M. (1992). Fluorescence lifetime imaging. *Analytical Biochemistry,* Vol. 202, No. 2, pp. 316-330, ISSN: 0003-2697

Lauterbur P. C. (1973). Image formation by induced local interactions: examples employing Nuclear Magnetic Resonance. *Nature,* Vol. 242, pp. 190-191

Louie A., Hüber M., Ahrens E., Rothbächer U., Moats R., Jacobs R., Fraser S. & Meade T. (2000). In vivo visualization of gene expression using magnetic resonance imaging. *Nature Biotechnology,* Vol. 18, pp. 321-325

Macrini T. E., Rougier G. W. & Rowe T. (2007). Description of a cranial endocast from the fossil mammal *Vincelestes neuquenianus* (Theriiformes) and its relevance to the evolution of endocranial characters in Therians. *The Anatomical Record: Advances in Integrative Anatomy and Evolutionary Biology,* Vol. 290, No. 7, pp. 875-892, ISSN: 1932-8494

Maddin H. C. (2011). Deciphering morphological variation in the braincase of caecilian amphibians (Gymnophiona). *Journal of Morphology,* Vol. 272, No. 7, pp. 850-871, ISSN: 1097-4687

Maisano J. A. & Rieppel O. (2007). The skull of the round Island boa, *Casarea dussumieri* Schlegel, based on high-resolution X-ray computed tomography. *Journal of Morphology,* Vol. 268, No. 5, pp. 371-384, ISSN: 1097-4687

Marino L., Uhen M. D., Pyenson N. D. & Frohlich B. (2003). Reconstructing cetacean brain evolution using computed tomography. *The Anatomical Record Part B: The New Anatomist,* Vol. 272B, No. 1, pp. 107-117, ISSN: 1552-4914

Metscher B. (2009). MicroCT for comparative morphology: simple staining methods allow high-contrast 3D imaging of diverse non-mineralized animal tissues. *BMC Physiology,* Vol. 9, No. 1, pp. 11, ISSN: 1472-6793

Moran P. (1986). The Acanthaster phenomenon. *Oceanography and Marine Biology,* Vol. 24, pp. 379-480

Neusser T., Heß M. & Schrodl M. (2009). Tiny but complex – interactive 3D visualization of the interstitial acochlidian gastropod *Pseudunela cornuta* (Challis, 1970). *Frontiers in Zoology,* Vol. 6, No. 1, pp. 20, ISSN: 1742-9994

Neves R. C., Sorensen K. J. K., Kristensen R. M. & Wanninger A. (2009). Cycliophoran dwarf males break the rule: high complexity with low cell numbers. *The Biological Bulletin,* Vol. 217, No. 1, pp. 2-5

Pawley J. B., (Ed(s).). (2006). *Handbook of biological confocal microscopy*, Springer Verlag, ISBN: 038725921X,

Radon J. (1917). Über die Bestimmung von Funktionen durch ihre Integralwerte längs gewisser Mannigfaltigkeiten. *Berichte der Sächsischen Akademie der Wissenschaften,* Vol. 69, pp. 262-278

Reits E. A. J. & Neefjes J. J. (2001). From fixed to FRAP: measuring protein mobility and activity in living cells. *Nature cell biology,* Vol. 3, No. 6, pp. 145-145, ISSN: 1465-7392

Ritman E. L. (2004). Micro-computed tomography-current status and developments. *Annual Review of Biomedical Engineering,* Vol. 6, pp. 185-208, ISSN: 1523-9829

Robb R. A. (1982). X-ray computed tomography: from basic principles to applications. *Annual review of biophysics and bioengineering,* Vol. 11, No. 1, pp. 177-201, ISSN: 0084-6589

Rogers S. W. (1999). Allosaurus, crocodiles, and birds: Evolutionary clues from spiral computed tomography of an endocast. *The Anatomical Record,* Vol. 257, No. 5, pp. 162-173, ISSN: 1097-0185

Ruffins S. W., Martin M., Keough L., Truong S., Fraser S. E., Jacobs R. E. & Lansford R. (2007). Digital three-dimensional atlas of quail development using high-resolution MRI. *TheScientificWorldJournal,* Vol. 7, pp. 592-604

Ruthensteiner B. & Heß M. (2008). Embedding 3D models of biological specimens in PDF publications. *Microscopy Research and Technique,* Vol. 71, No. 11, pp. 778-786, ISSN: 1097-0029

Salisbury J. (1994). Three-dimensional reconstruction in microscopical morphology. *Histology and histopathology,* Vol. 9, No. 4, pp. 773-780, ISSN: 0213-3911

Schreurs G., Hänni R., Panien M. & Vock P. (2003). Analysis of analogue models by helical X-ray computed tomography. *Geological Society, London, Special Publications,* Vol. 215, No. 1, pp. 213-223

Sekar R. B. & Periasamy A. (2003). Fluorescence resonance energy transfer (FRET) microscopy imaging of live cell protein localizations. *The Journal of Cell Biology,* Vol. 160, No. 5, pp. 629-633

Streicher J. & Müller G. B. (2001). 3D modelling of gene expression patterns. *Trends in biotechnology,* Vol. 19, pp. 145-148

Stuppy W. H., Maisano J. A., Colbert M. W., Rudall P. J. & Rowe T. B. (2003). Three-dimensional analysis of plant structure using high-resolution X-ray computed tomography. *Trends in Plant Science,* Vol. 8, No. 1, pp. 2-6, ISSN: 1360-1385

Thevenaz P., Ruttimann U. E. & Unser M. (1998). A pyramid approach to subpixel registration based on intensity. *Image Processing, IEEE Transactions on,* Vol. 7, No. 1, pp. 27-41, ISSN: 1057-7149

Ustione A. & Piston D. W. (2011). A simple introduction to multiphoton microscopy. *Journal of Microscopy,* Vol. 243, No. 3, pp. 221-226, ISSN: 1365-2818

Vasquez S. X., Hansen M. S., Bahadur A. N., Hockin M. F., Kindlmann G. L., Nevell L., Wu I. Q., Grunwald D. J., Weinstein D. M., Jones G. M., Johnson C. R., Vandeberg J. L., Capecchi M. R. & Keller C. (2008). Optimization of volumetric computed tomography for skeletal analysis of model genetic organisms. *The Anatomical Record: Advances in Integrative Anatomy and Evolutionary Biology,* Vol. 291, No. 5, pp. 475-487, ISSN: 1932-8494

Verraes W. (1974). Notes on the graphical reconstruction technique. *Biologisch Jaarboek Dodonaea,* Vol. 42, pp. 182-191

Vlaardingerbroek M. T. & Den Boer J. A. (2003). *Magnetic resonance imaging: theory and practice*. Springer Verlag, ISBN: 3540436812,

Walter T., Shattuck D. W., Baldock R., Bastin M. E., Carpenter A. E., Duce S., Ellenberg J., Fraser A., Hamilton N. & Pieper S. (2010). Visualization of image data from cells to organisms. *Nat Methods,* Vol. 7, No. 3 Suppl, pp. S26-S41

Wanninger A. (2007). The application of confocal microscopy and 3D imaging software in Functional, Evolutionary, and Developmental Zoology: reconstructing myo-and neurogenesis in space and time, In: *Modern Research and Educational Topics in Microscopy*, A., M.-V., et al., pp. 468, Formatex, Bardajoz, Spain

Wanninger A. (2009). Shaping the things to come: ontogeny of lophotrochozoan neuromuscular systems and the Tetraneuralia concept. *The Biological Bulletin,* Vol. 216, No. 3, pp. 293-306

Wirkner C. S. & Prendini L. (2007). Comparative morphology of the hemolymph vascular system in scorpions – A survey using corrosion casting, MicroCT, and 3D-reconstruction. *Journal of Morphology,* Vol. 268, No. 5, pp. 401-413, ISSN: 1097-4687

Yang H. F. & Choe Y. (2009). Cell tracking and segmentation in electron microscopy images using graph cuts. *Proceedings of IEE International Symposium on Biomedical Imaging: from Nano to Macro,* ISBN: 1945-7928, Boston, MA, August 2009

Ziegler A., Faber C., Mueller S. & Bartolomaeus T. (2008). Systematic comparison and reconstruction of sea urchin (Echinoidea) internal anatomy: a novel approach using magnetic resonance imaging. *BMC Biology,* Vol. 6, No. 1, pp. 33, ISSN: 1741-7007
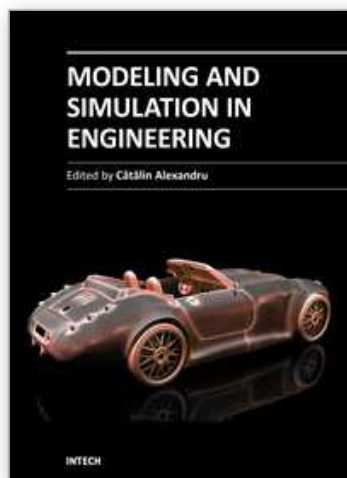
Modeling and Simulation in Engineering
Edited by Prof. Catalin Alexandru

This book provides an open platform to establish and share knowledge developed by scholars, scientists, and engineers from all over the world, about various applications of the modeling and simulation in the design process of products, in various engineering fields. The book consists of 12 chapters arranged in two sections (3D Modeling and Virtual Prototyping), reflecting the multidimensionality of applications related to modeling and simulation. Some of the most recent modeling and simulation techniques, as well as some of the most accurate and sophisticated software in treating complex systems, are applied. All the original contributions in this book are jointed by the basic principle of a successful modeling and simulation process: as complex as necessary, and as simple as possible. The idea is to manipulate the simplifying assumptions in a way that reduces the complexity of the model (in order to make a real-time simulation), but without altering the precision of the results.

How to reference
In order to correctly reference this scholarly work, feel free to copy and paste the following:

Christian Laforsch, Hannes Imhof, Robert Sigl, Marcus Settles, Martin Heß and Andreas Wanninger (2012). Applications of Computational 3D–Modeling in Organismal Biology, Modeling and Simulation in Engineering, Prof. Catalin Alexandru (Ed.), ISBN: 978-953-51-0012-6, InTech, Available from: http://www.intechopen.com/books/modeling-and-simulation-in-engineering/applications-of-computational-3d-modeling-in-biological-sciences

INTECH
open science | open minds